Bioelectrochemistry 135 (2020) 107583

Contents lists available at ScienceDirect

Bioelectrochemistry

journal homepage: www.elsevier.com/locate/bioelechem

Dielectric properties of healthy and diabetic alloxan-induced lenses in rabbits

E. Marzec [a,*], M. Nowakowska De Rossi [b], S. Paolucci [b], J. Olszewski [a]

[a] Department of Bionics and Bioimpedance, Poznan University of Medical Sciences, Parkowa 2, 60–775 Poznań, Poland
[b] Institute Santa Lucia Foundation IRCCS, Neurosciences and Rehabilitation, Via Ardeatina 306, 00179 Roma, Italy

ARTICLE INFO

Article history:
Received 27 March 2020
Received in revised form 3 June 2020
Accepted 3 June 2020
Available online 9 June 2020

Keywords:
Diabetic lens
Activation energy
Dielectric properties

ABSTRACT

The dielectric properties of the eye lens were studied for healthy and alloxane-induced diabetic rabbits in the frequency range from 500 Hz to 100 kHz electric field and temperatures from 25 to 50 °C. In the full temperature range, the average relative permittivity and dielectric loss values for a healthy lens are lower than those recorded for diabetic tissue. Dielectric relaxation of polar amino acids on the alpha-crystallin surface with a characteristic frequency of 7 kHz in the range of 25–50 °C for healthy and diabetic samples is accompanied by the activation energy of proton conductivity with an average values of 33 and 39 kJ mol^{-1}, respectively. The permittivity decrement, which characterizes the size of the dielectric dispersion with a central relaxation time of 0.023 ms for a diabetic sample, is more than twice as high as for a healthy sample. Measurements on the rabbit eye lens were carried out at ambient temperature above and below the physiological range, since these conditions provide an appropriate pattern of dielectric behavior for the diagnosis of clinical dysfunction of the human lens.

1. Introduction

The influence of external factors such as relative humidity, temperature and electromagnetic radiation on the human and animal lens can modify the normal functioning of the tissue such as its transparency, refraction, plasticity and other important features that determine the quality of the optical signal received by the retina. Experimental methods provide information on the physical properties of the lens such as thermal [1,2], optical [3–6], mechanical [7,8] and electrical [9–16] processes occurring at the molecular level of the lens, which reflect the functioning of healthy and physiologically disturbed tissue. Physical and chemical research on the lens [17–20] has proven the key role of water in maintaining the proper structure of crystallins, a unique group of water-soluble proteins that represent a high level of the total weight of the lens in the eye of mammals. Water, which has a high dielectric permittivity and the ability to form specific bonds, most strongly affects the electrical conductivity of ions or protons in the structural layers of the lens. Reduced water transport through all layers of the lens causes protein aggregation, which affects the quality of eye vision. Therefore, maintaining intralenticular solubility and preventing the aggregation of proteins depends on the activity of adenosine triphosphate (ATP), the α-crystallin molecule as a chaperone and the cell membrane of the lens [11,18,21].

The main purpose of this study was to extend our previous *in vitro* dielectric measurement of rabbit lenses [22] with further investigation to the *in vivo* alloxan-induced diabetic lens in these animals. This is in line with the procedure for causing hyperglycemia in experimental animals by streptozotocin (STZ) or alloxan. Various studies conducted in the eyes of humans and animals [23–27] describe changes associated with diabetes in the structure-function relationship of the lens. Differences between healthy and diabetic lenses occur in every structural element of this biological material and result from abnormal glucose metabolism affecting the physiological properties of the lens. In our studies using dielectric spectroscopy in the α-dispersion region of the electric field we can analyze the relationship between the molecular structure and the electrical response of a diabetic lens in a rabbit. In addition, the simultaneous effect of electric field and temperature on tissue during measurements allowed us to compare differences in the mechanism of electrical conductivity, reflecting the mobility and density of charge carriers between the healthy and diabetic lens, caused by the thermal interaction of water with protein particles. To perform these tests, we varied the lens ambient temperature in the measuring chamber [28] at values above and below the physiological range, because these conditions provide an appropriate dielectric behavior pattern for

* Corresponding author.
E-mail address: ewaklcde@amu.edu.pl (E. Marzec).

https://doi.org/10.1016/j.bioelechem.2020.107583
1567-5394/

the clinical diagnosis of human lens dysfunction. Dielectric spectroscopy can also be used in a non-invasive way to assess changes in the structural proteins of the human lens due to diseases such as cataracts, diabetic retinopathy, and presbyopia. These initial measurements can be helpful in identifying a patient who requires early clinical intervention procedures.

However, *in vivo* responses to the applied electric field to the electrode-lens system depend not only on the structural phases of this tissue, as in the state of *in vitro*, but also on the endogenous electrical activity of ions between the aqueous humor and the lens. As a result, it is difficult to accurately assess the magnitude of polarization and conduction of electrical processes in the lens *in vivo*, especially as a function of time. In turn, the next goal of our research was to use the *in vitro* dielectric method to discover drugs or test them on the lenses of rabbits. Therefore, as an example, it was necessary to test diabetic rabbit lens *in vitro* treated with vitamin K1 to compare the dielectric properties of samples prepared in this way healthy lens samples. The data obtained was intended to enable assessment of the role of vitamin K1 as an anti-cataract agent inhibiting glycation in the lens [26].

2. Materials and methods

In vitro studies of the dielectric properties of lens samples were performed for a healthy group of 6 rabbits and an experimental group of 6 alloxan-induced diabetic rabbits. Each group comprised male animals of 6 months age weighing approximately 3.5 kg. The experimental group received an intravenous injection of alloxan into an ear vein to induce diabetes achieving blood glucose levels in the range 25–31 mmol/L. All animals were euthanised at three months. The lens was immediately excised and immersed in 0.9% NaCl. Prior to dielectric measurements, lenses were washed with distilled water, dried at room temperature and then each lens (mass ~ 200 mg) compressed at ~ 2 MPa into a disk with a diameter of 10 mm and a thickness of 1 mm. This mechanical process modified the complex fiber system of the lens tissue to give an isotropic structure which also does not contain trapped air which could affect the dielectric measurement. The resulting disks were cut into about four rectangular samples with dimensions of about 3 mm × 5 mm × 1 mm.

These solid state samples, with an average water content of 6% [22], corresponded to room temperature air dried samples produced at a relative humidity of about 70%. A feature of air dried samples is the balance of hydration between them and the external environment. Therefore, to assess the water content of air dried samples, several healthy and diabetic samples, except for those intended for dielectric experiment, were placed in a measuring chamber and the experiment started in the same way as for a rabbit lens in our earlier article [22]. During this experiment, the samples were heated for 1 h at 150 °C, and then cooled to room temperature, removed from the chamber, weighed, and their weight loss relative to their weight before measurement corresponded to the water content of these samples. In order to reduce the polarization of electrodes during electrical measurements, it was necessary to apply thin layer electrodes to the sample surface. As a result, across the electrode-tissue system, electrode capacitance could be high compared to lens capacitance. To prepare thin film electrodes, two surfaces of the test sample were covered with a small amount of silver paste using a miniature spatula. According to this procedure, the electrode layer dries quickly due to evaporation of solvents and chemicals present in the paste. After completing this preparatory procedure, the finished sample-electrode laminate was placed in a measuring chamber [28] and the dielectric experiment started. The dielectric properties of healthy and diabetic lenses were obtained on the basis of electrical resistance (R) and capacity (C) measurement as parameters, also taking into account the geometry of the sample. Measurements of R and C were carried out using an impedance analyser (HIOKI 3522–50 LCR) over the frequency range, f, of 500 Hz-100 kHz and at temperatures, T, from 25 to 50 °C. The values for relative permittivity ε', dielectric loss ε'' and conductivity σ in these samples were calculated from $\varepsilon' = Cd/\varepsilon_o S$, $\varepsilon'' = d/\omega\varepsilon_o RS$ and $\sigma = \omega\varepsilon_o\varepsilon''$, where d = 1 mm and S = 15 mm^2 are the inter-electrode distance and electrode area, respectively, ε_o is the permittivity of a vacuum (ε_o = 8.854 pF/m), and ω is the angular frequency ($\omega = 2\pi f$).

The values of the dielectric parameters for each group of healthy and diabetic samples are given as the average of 10 measurements (n = 10) with a coefficient of variation (CV) for reproducibility of 5%.

3. Results and discussion

Fig. 1 shows the temperature dependence of the loss tangent, tan δ (=$\varepsilon''/\varepsilon'$), for a healthy and diabetic rabbit lens at selected frequencies of 2 and 25 kHz.

These data reflect the electrical differences between the structural layers of the lens tissue, such as capsule, epithelium, cortex and nucleus, which determine the activity of hydrated water. Therefore, in the temperature range 25–50 °C for both tested lens types (Fig. 1), changes in tan δ values were the result of different concentrations of water interacting with the surfaces of the component phases in the capsule-epithelium-cortical system and in the cortical-nuclear system of bulk tissue, respectively. Studies of human and animal eye lenses using various types of magnetic resonance imaging (MRI) [29–31] have shown that there is a change in the ratio of water to protein defined as the gradient refractive index (GRIN) in these tissues that are lowest at the perimeter of the lens and then increase towards the center, hence the water content is highest in the outer cortex and lowest in the nucleus.

This variation correlates with the internal microcirculation system of the lens [32] designed to maintain ionic, fluid, and metabolite homeostasis in the tissue, which determines transparency and GRIN. As a result of an increase in temperature (Fig. 1), the network of hydrogen bonds breaks around the structural layers of the lens, a greater number of freely relaxing polar sites results and surrounding ions are created, which in turn increases the dissipation of electricity in the form of heat. Another study [1] using low angle X-rays on rabbit lens, performed between 20 and 70 °C, showed that temperature-induced structural change in this tissue is caused by an increased disruption that corresponds to thermodynamic entropy.

The results in Fig. 1 also show that at each temperature, the tan δ values decrease for the two samples types in response to the increasing frequency of the electric field from 2 to 25 kHz. This is

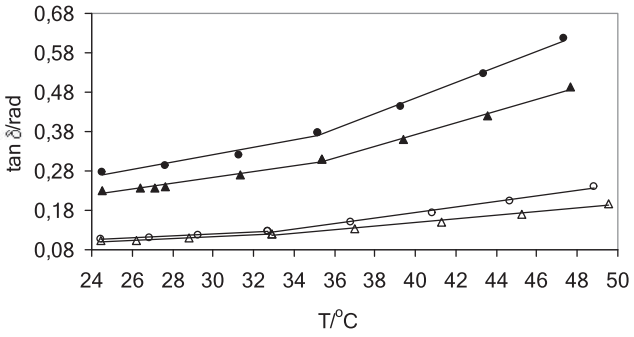

Fig. 1. Temperature dependencies of tan δ for healthy and diabetic rabbit lens at 2 kHz (▲: healthy; ●: diabetic) and 25 kHz (Δ: healthy; ○: diabetic). For each point n = 10.

the effect of shortening the orientational relaxation times, τ, of polar side groups on the protein surface. Thus, the τ value of 6 μs at about 25 kHz is thirteen times shorter than the value of τ = 80 μs at about 2 kHz for the dielectric spectra shown in Fig. 1. In addition, reduction in the translation time of water protons that hop between the polar sites of the component phases of the lens tissue is also due to the increase in frequency from 2 to 25 kHz. Recently, dielectric spectroscopy studies of hydrated powdered proteins with various protein morphologies have also been interpreted through the process of proton hopping in water [33].

The main proteins in the capsule and in the other phases of the lens are collagen IV and crystallin, respectively. According to literature data [34], polar sites in collagen IV are associated with positive amino groups and negative carboxyl groups of the side chains in the main amino acids of the lens capsule, such as lysine (Lys), hydroxylysine (Hyl) and arginine (Arg), and glutamic acids (Glu). In the case of crystallin, the polar sites are associated with α-crystallin, the main protein fraction in the lens of the eye shown in Fig. 2, as a well-characterized α-crystallin amino acid sequence.

This illustrates the clear distinction between amino acids with electrically charged side groups and other amino acids. The number of amino acids with Arg, histidine (His) and Lys basic charged side groups and with the acid side groups of aspartic acid (Asp), glutamic acid (Glu) and tyrosine (Tyr) are 27 and 31, respectively. In turn, Fig. 3 shows the chemical reactivity of selected fragments of α-crystallin with charged (Arg, His, Glu, Lys) and polar, i.e., glutamine (Gln), asparagine (Asn), cysteine (Cys) and non-polar, i.e., phenylalanine (Phe), glycine (Gly), proline (Pro), isoleucine (Ile) amino acids.

The numerous observed hydrogen bonds that are formed between α-crystallin residues and water molecules form a favorable network for the proton conduction process, which becomes obvious in respect to dielectric behavior.

Alloxane-treated rabbits showed changes in dielectric properties. This is indicated by the curves in Fig. 1, where there is a clear difference in the dielectric behavior of diabetic and healthy tissue samples in the range 25–50 °C. For a diabetic sample, tan δ values at 2 and 25 kHz are higher than those obtained for a healthy sample. The gap of loss tangent between healthy and diseased samples increases with temperature, presumably due to a glycation effect, which will lead to the greater release of protons through breaking of hydrogen bonds formed by water on the surface of the protein molecules. The glycation reaction involves a number of steps. The first stage occurs between glucose carbonyl groups and free amino groups on proteins. This reaction usually proceeds with the amino group of Lys residues, which leads to the next step associated with the formation of the initial Schiff base, which is converted to a more stable Amadori product, which then undergoes further reactions with dicarbonyl intermediates. This leads to the final stage of the formation of advanced glycation end-products (AGEs) [21,24,25], e.g., pentosidine, as shown in Schematic 1. Pentosidine is a cross-link formed between Lys and Arg residues on the α-crystallin surface [35].

MDVTIQHPWF KRTLGPFYPS RLFDQFFGEG LFEYDLLPFL SSTISPYYRQ
SLFRTVLDSG ISEVRSDRDK FVIFLDVKHF SPEDLTVKVQ DDFVEIHGKH
NERQDDHGYI SREFHRRYRL PSNVDQSALS CSLSADGMLT FCGPKIQTGL
DATHAERAIP VSREEKPTSA PSS

Fig. 2. α-crystallin sequence with 173 amino acid residues. Black indicates the charged amino acids Arg (R), His (H), Lys (K), Asp (D), Glu (E) and Tyr (Y) in quantities 13, 7, 7, 15, 10 and 6, respectively, in total fifty-eight.

A study of diabetic animal lenses [36,37] indicates that a marked increase in pentosidine and AGE depends on the glycemic threshold. However, the participation of the basic Lys and Arg side groups in the chemical glycation process prevents the formation of a hydrogen bond of water molecules with these groups. As a consequence, this water can form many hydrogen bonds with other water molecules. Therefore, such water behavior can be reflected in Fig. 1 using curves indicating that the number of proton jumps producing electric energy dissipation will be greater in diabetic samples, and this gap tan δ is quite pronounced at f = 2 kHz with an electric field period (1/f) longer than that at f = 25 kHz. Because tan δ indicates the ratio of lost electricity (reflected in ε″) to energy saved (reflected in ε′) in both materials, the parameters ε′ and ε″ are presented as a function of temperature for 2 and 25 kHz in Fig. 4(a). These graphs compare the dielectric behavior of the samples tested in relation to the mechanism of interfacial polarization and conduction of ions and protons between the phases of heat - treated lens. The values of ε′ and ε″ depend respectively on the number of relaxing polar sites available for the accumulation of charge carriers and the number of charges moving freely between these sites, respectively. The effect of glycation on the ε′ and ε″ of the lens at any temperature in Fig. 4(a) confirms 2–3 fold higher values for these parameters than those recorded for healthy samples at 2 and 25 kHz. This is due to the higher density of polar sites in the diabetic lens, which affects the surface charge of the protein-glucose system under the influence of an electric field. In addition, both ε′ and ε″ data for a diabetes sample in the range of 25–50 °C show that ion or proton conduction dominates the interfacial polarization, an effect confirmed in Fig. 1 with a greater slope of the tan δ graph than for a healthy sample, especially above 30 °C.

To analyze the mechanism of electrical conduction associated with the movement of protons in the protein-water system of a healthy and diabetic lens, the Arrhenius plots of conductivity, σ, versus the inverse of temperature, T^{-1} at 2 and 25 kHz are shown in Fig. 4(b). The Arrhenius equation with Boltzmann energy (kT) in the form $\sigma = \sigma_o \exp(\Delta H/kT)$, where σ_o is the pre-exponential factor, and ΔH is the activation energy, is appropriate to characterize the proton-hopping process between polar sites. The ΔH values for each curve were obtained

from the slope of the straight line for the temperature range from 3.35 K^{-1} (25 °C) to 3.09 K^{-1} (50 °C). As the temperature rises, the density of protons increases in both samples as a result

of the reorientation and breaking of the hydrogen bonded network around the protein molecules with a minimum of ΔH. The σ values for the diabetic samples at any temperature are higher than the values recorded for healthy samples as a result of the increase in hydrogen-bound networks between the surface of the structural tissue phases and this in turn causes an increase in proton mobility correlated with shorter distance between sites that can be occupied by jumping protons.

Arrhenius analysis in Fig. 4(b) showed that for healthy and diabetic samples ΔH values at 2 kHz are 0.41 eV (40 kJ mol^{-1}) and 0.45 eV (44 kJ mol^{-1}) and fall to 0.30 eV (29 kJ mol^{-1}) and 0.36 eV (35 kJ mol^{-1}) at 25 kHz. The differences in ΔH between both materials indicate that more energy is needed in the diabetic sample to release not only protons that would also be present in a healthy sample but also additional chemical components such as AGEs in the modified protein-water lens system. Our previous *in vitro* studies [38] on the nail plate have also shown that hyperglycemia causes an increase in ΔH conductivity compared to non-diabetic nails. However, in the range 25–60 °C, for example, at 2 kHz, ΔH = 25 kJ mol^{-1} and ΔH = 34 kJ mol^{-1} for healthy and diabetic nails, respectively, are lower than those obtained for the eye lens. This behavior may be due to the lower density of polar sites and protons in the nail, resulting from other structural elements than in the lens.

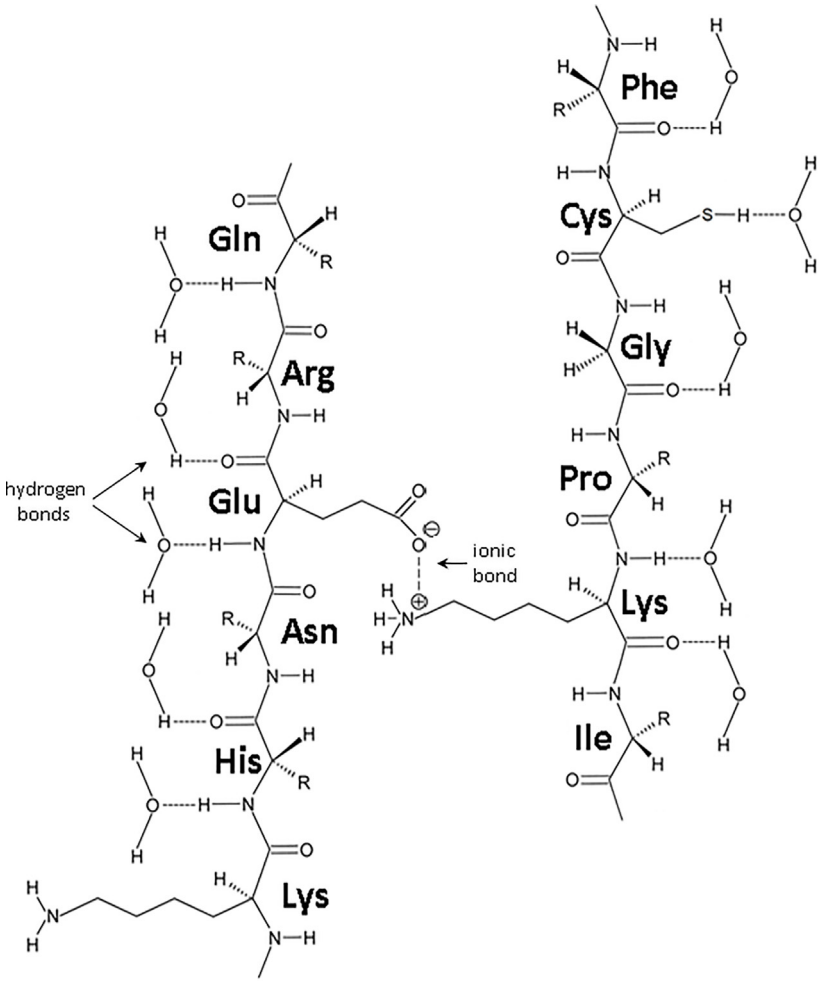

Fig. 3. Schematic representation of α-crystallin with a 6 amino acid fragment at positions 99–104 (KHNERQ) and 141–146 (FCGPKI). KHNERQ and FCGPKI refer to the peptide Lys-His-Asn-Glu-Arg-Gln and Phe-Cys-Gly-Pro-Lys-Ile according to Fig. 2. An example of hydrogen bonds (••••••) and ionic bond (– – –).

Schematic 1 also shows S-S disulfide bonding between the side chains of two cysteine residues as a result of non-enzymatic glycation. Because polar amino acid residues are mainly found on the surface of protein molecules [39], so also cross-linking of Lys-Arg and Cys-Cys residues on the surface of α-crystallin molecules can affect the capsule-epithelium-cortex-nucleus interaction with water. However, the differences between the dielectric behavior obtained in these two materials may depend mainly on the cortex and nucleus. This is due to the distribution of protein density in the lens of the eye, which is the lowest in the periphery and increases towards the center of the lens [40,41]; this behavior is accompanied by a decrease in water content. Consequently, a greater contribution to the dielectric response will come from the cortical zone.

Fig. 5(a and b) shows a comparative analysis of the frequency dependence on the parameters ε′, ε″ and σ for both materials in the full frequency range from 500 Hz to 100 kHz electric field at a temperature of 36 °C, which corresponds to physiological conditions.

These spectra illustrate that the effect of glycation on the lens leads to an increase in the dielectric properties of this tissue, which in turn affects the intensity of polarization and conduction processes also observed in Fig. 4 at two selected frequencies in the range of 25–50 °C. Data obtained below and above 2 kHz in Fig. 5(a) are due to interfacial polarization between the absorbed water and the polar region of the protein surface in the capsule-epithelium-cortex system and in the cortex-nucleus system of bulk tissue, respectively. In addition, the interfacial polarization in these two frequency ranges correlates with conductivity, the value of which is almost constant to 2 kHz, and then increases rapidly above 2 kHz for both samples, as shown in Fig. 5(b). Thus, the effect of water on the dielectric parameters below 2 kHz in Fig. 5(a) is interpreted as low frequency dispersion (LFD) in the form $\varepsilon' \sim f^{-n}$ and $\varepsilon'' \sim f^{-k}$ with exponents n = 0.2 and k = 0.6. However, these spectra show that a similar slope for both samples is associated with a higher density of polar sites and free ions or protons between the surfaces of the structural layers of the diabetic lens compared to the healthy lens.

Results above 2 kHz in Fig. 5(a and b) are interpreted using the Cole-Cole function:

$$\varepsilon^* = \varepsilon_h + \frac{\Delta\varepsilon}{1 + (j\omega\tau)^{(1-\alpha)}} \quad (1)$$

Where ε^* ($\varepsilon^* = \varepsilon' - j\varepsilon''$) is the complex permittivity, ε_h is the high-frequency limit of relative permittivity at 100 kHz, $\Delta\varepsilon$ is permittivity decrement characterizing the magnitude of dielectric dispersion, τ is the relaxation time ($\tau = 1/2\pi f_c$), f_c is the characteristic frequency, and α denotes the degree of broadening of the dispersion spectra. Previously, the Cole-Cole equation was also used to study the electrical properties of frog [13] and goat [14,15] lenses in the range from 500 Hz to 500 MHz and from 10 mHz to 10 Hz, respectively. These results show the characteristic frequency f_c for a frog at 2 kHz and 2 MHz, and at 1 Hz for a goat.

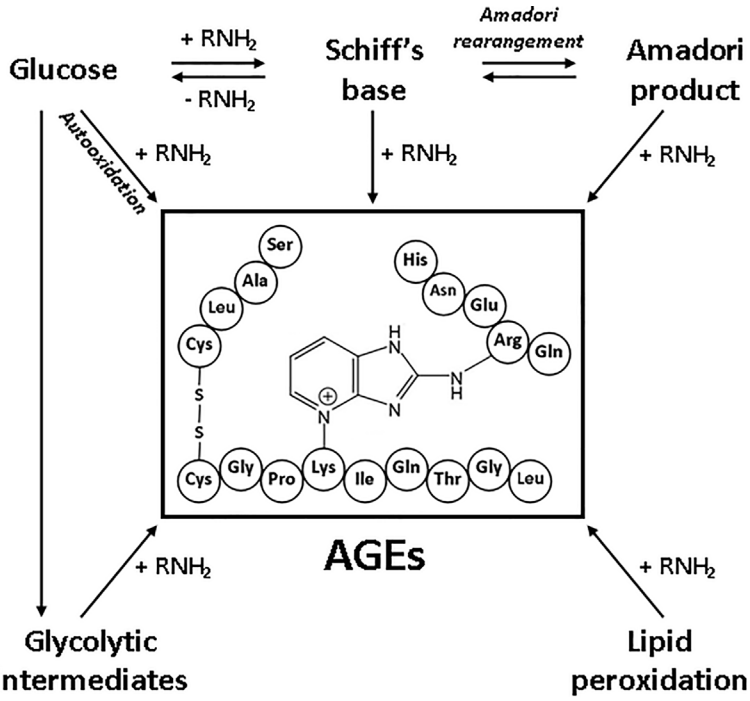

Schematic 1. Scheme of pentosidine formation as one of the advanced glycation end products (AGEs) of the crystalline fragment.

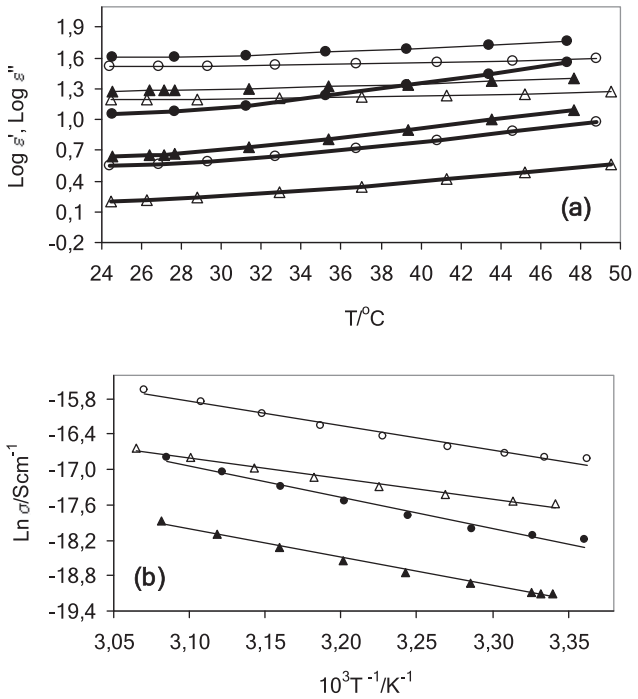

Fig. 4. Temperature dependencies of **(a)** log ε' and log ε″, and **(b)** Arrhenius plots of ln σ for healthy and diabetic rabbit lens at 2 kHz (▲: healthy; ●: diabetic) and 25 kHz (Δ: healthy; ○: diabetic). Thin and bold lines in **(a)** indicate ε′ and ε″, respectively.

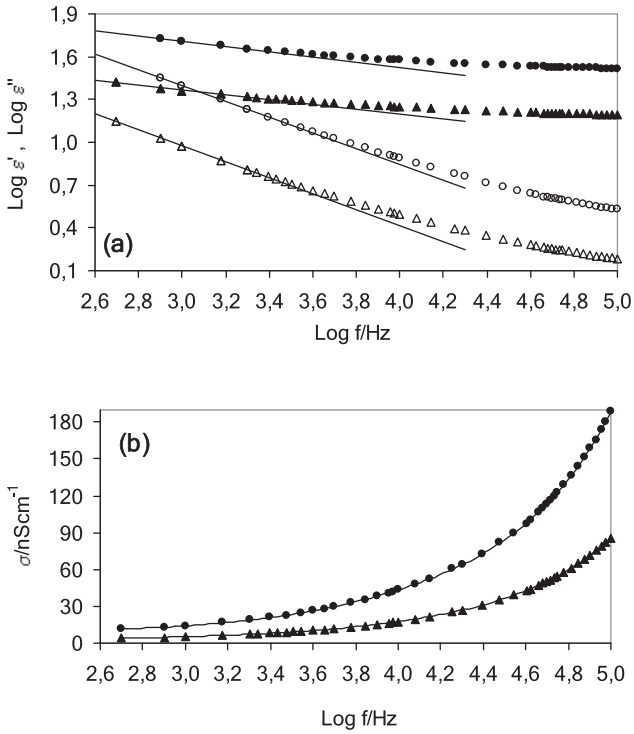

Fig. 5. Frequency dependencies of **(a)** log ε′ (▲: healthy; ●: diabetic) and log ε″ (Δ: healthy; ○: diabetic), and **(b)** σ (▲: healthy; ●: diabetic) for healthy and diabetic rabbit lens at 36 °C. Solid lines in **(a)** indicate low frequency dispersion (LFD).

To study the differences between healthy and diabetic tissues, based on the results above 2 kHz at 36 °C (Fig. 5) are shown in Fig. 6 plots of ε″ against ε′ as a Cole-Cole representation also at 25 and 45 °C.

To obtain these spectra, it was assumed that σ_l is the low frequency conductivity limit at 2 kHz, so the dielectric loss ε″ (imaginary parts ε*) is given as $(\sigma-\sigma_l)/\omega\varepsilon_o$. The value of Δε increases with increasing temperature in the range of 25–45 °C for healthy and diabetic tissues. For both samples, these data show semicircular behavior with one characteristic frequency f_c of about 7 kHz (τ = 23 μs), which appears to be independent of temperature. For comparison, in the 0.2–20 GHz frequency range in aqueous

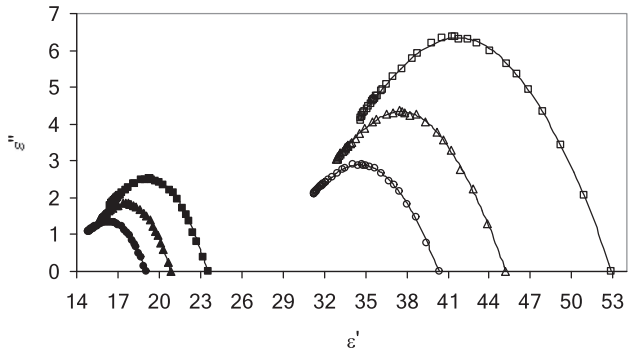

Fig. 6. Cole-Cole plots of ε″ against ε′ for healthy (●: 25 °C, ▲: 36 °C and ■: 45 °C), and diabetic (○: 25 °C, Δ: 36 °C and □: 45 °C) rabbit lens.

Table 1
Dielectric parameters Δε, Δσ and α for healthy (n = 10) and diabetic (n = 10) groups at 25 °C, 36 °C and 45 °C, and in the range of 2–100 kHz.

lens	T/°C	Δε	Δσ/nS cm^{-1}	α
healthy	25	4	59	0.63
diabetic	25	9	117	0.50
healthy	36	5	79	0.57
diabetic	36	12	169	0.46
healthy	45	7	99	0.62
diabetic	45	18	229	0.48

solutions at room temperature, the amino acid as the basic structural element of the protein has a relaxation time τ, which corresponds to a picosecond time scale [42,43]. Examples of this are Lys, Arg and Gly, with τ values 127.6, 159.9 and 33.4 ps, respectively. This means that low molecular weight Lys (146 Da), Arg (174 Da) and Gly (75 Da) determine the shorter τ in response to the applied electric field than α-crystallin with a molecular weight in the range from 300 to over 1000 kDa [44]. As shown in Fig. 6, differences in dielectric behavior between these two sample types showed as higher spectra in diabetic compared to healthy samples. This indicates that, as below 2 kHz, the diabetic lens response to an electric field in the range of 2–100 kHz is also greater in crystallin-glucose-water complexes in bulk tissue than in the case of the non-diabetic lens. In addition, the process of relaxation of polar residues on the protein surface at f_c = 7 kHz in the range of 25–45 °C for healthy and diabetic samples is accompanied by the calculated activation energy ΔH of proton conductivity of f_c, 33 kJ mol^{-1} and 39 kJ mol^{-1}, respectively. Therefore it means, that for diabetic samples, due to the possible increase in the number of hydrogen bonds formed by water, a higher ΔH value is needed to break these bonds with an increase in temperature compared to healthy samples. Table 1 compares for both samples in the range of 2–100 kHz, the magnitude of relaxation Δε and Δσ (=σ − $σ_l$), as well as the parameter α obtained from the fitted curves to Eq. (1) in Fig. 6.

The data in Table 1 show that at 25, 36 and 45 °C the values of Δε and Δσ dielectric dispersion with a central relaxation time of τ = 23 μs (f_c = 7 kHz) for a diabetic sample are more than two times higher than the values shown by a healthy sample. This indicates that hyperglycemia causes an increase in the number of relaxing active sites and free protons in lens protein molecules. For the analyzed dispersion of both samples, the Cole-Cole parameter α in the range of 0.46–0.63 showing a broad distribution of relaxation times is the result of differences in the molecular density of crystalline and water in the bulk cortical-nuclear system. Thus, in the cortical region, the intensity of interfacial polarization decreases to a minimum in the nuclear region due to the reduction in the size of polar surfaces involved in the ion and proton charging process. The nucleus region consists of more closely packed crystalline molecules with a lower water content than in the cortex. The more diffuse intermediate zone between the cortex and the nucleus can, accordingly, be considered the interface responsible for the observed wide distribution of the relaxation behavior of the lens.

4. Conclusion

The effect of glycation on the dielectric parameters of the lens at any temperature is the result of a greater number of polar sites than in a healthy sample, which affects the mechanism of polarization of protein molecules on the surface and within this tissue under the influence of an electric field. Similarly, the mechanism of electrical conductivity associated with the movement of protons or ions is more intense in diabetic lenses compared to healthy tissue due to the non-enzymatic glycation of α-crystallin molecules mainly using Lys and Arg residues. Hyperglycemia causes an increase in conduction activation energy compared to a non-diabetic lens, indicating that additional energy is needed to release electric charge carriers between the advanced glycation end-products (AGEs). Based on dielectric measurements of the diabetic lens in rabbits, it is possible to identify proton conduction and interfacial polarization, two important relaxing processes that will also affect the physiological integrity of the human lens. Our working hypothesis, in relation to planned dielectric measurements on powdered human healthy and diabetic cadaveric lens, is that glycation leads to an increase in the dielectric properties of the human lens, as in the case of the rabbit lens. In addition, further lens testing is needed to determine if there is a surface roughness effect due to tissue powdering in these dielectric measurements. Such future studies should also confirm whether the preparation of a solid sample from powder form has the same integrity and effect on dielectric measurement as the solid rabbit lens.

Declaration of Competing Interest

None.

References

[1] J.W. Regini, J.G. Grossmann, M.R. Burgio, N.S. Malik, J.F. Koretz, S.A. Hodson, G. F. Elliott, Structural changes in α-crystallin and whole eye lens during heating, observed by low-angle X-ray diffraction, J. Mol. Biol. 336 (2004) 1185–1194.
[2] K.R. Heys, M.G. Friedrich, R.J.W. Truscott, Presbyopia and heat: changes associated with aging of the human lens suggest a functional role for the small heat shock protein, α-crystallin, in maintaining lens flexibility, Aging Cell 6 (2007) 807–815.
[3] B. Pierscionek, M. Bahrami, M. Hoshino, K. Uesugi, J. Regini, N. Yagi, The eye lens: age-related trends and individual variations in refractive index and shape parameters, Oncotarget 6 (2015) 30532–30544.
[4] W.K. Lo, S.K. Biswas, L. Brako, A. Shiels, S. Gu, J.X. Jiang, Aquaporin-0 targets interlocking domains to control the integrity and transparency of the eye lens, Invest. Ophthalmol. Vis. Sci. 55 (2014) 1202–1212.
[5] E. Vaghefi, A. Kim, P.J. Donaldson, Active maintenance of the gradient of refractive Index is required to sustain the optical properties of the lens, Invest. Ophthalmol. Vis. Sci. 56 (2015) 7195–7208.
[6] M. Breea, D. Borchman, The optical properties of rat, porcine and human lenses in organ culture treated with dexamethasone, Exp. Eye Res. 170 (2018) 67–75.
[7] Q. Wang, Y. Zhu, M. Shao, H. Lin, S. Chen, X. Chen, A. Alizad, M. Fatemi, X. Zhang, In vivo assessment of the mechanical properties of crystalline lenses in a rabbit model using ultrasound elastography: Effects of ultrasound frequency and age, Exp. Eye Res. 184 (2019) 258–265.
[8] R. Michael, R.I. Barraquer, B. Willekens, J. van Marle, G.F. Vrensen, Morphology of age-related cuneiform cortical cataracts: the case for mechanical stress, Vision Res. 48 (2008) 626–634.
[9] M. Zhao, L. Chalmers, L. Cao, A.C. Vieira, M. Mannis, B. Reid, Electrical signaling in control of ocular cell behaviors, Prog. Retin. Eye Res. 31 (2012) 65–88.
[10] R.T. Mathias, J. Kistler, P. Donaldson, The lens circulation, J. Membr. Biol. 216 (2007) 1–16.
[11] N.J. Ray, Biophysical chemistry of the ageing eye lens, Biophys. Rev. 7 (2015) 353–368.
[12] S. Bassnett, Y. Shi, G.F.J.M. Vrensen, Biological glass: structural determinants of eye lens transparency, Phil. Trans. R. Soc. B 366 (2011) 1250–1264.

[13] M. Watanabe, T. Suzaki, A. Irimajiri, Dielectric behavior of the frog lens in the 100 Hz to 500 MHz range. Simulation with an allocated ellipsoidal-shells model, Biophys. J. 59 (1991) 139–149.
[14] D.V. Rai, K.S. Kohli, Impedance of goat lens as a function of frequency at DC voltages 0, 50, 100, 200 mV, Electromagn. Biol. Med. 25 (2006) 155–162.
[15] K.S. Kohli, D.V. Rai, P. Kumar, V.K. Jindal, N. Goyal, Impedance of a goat eye lens, Med. Biol. Eng. Comput. 35 (1997) 348–353.
[16] G. Schmid, R. Überbacher, Age dependence of dielectric properties of bovine brain and ocular tissues in the frequency range of 400 MHz to 18 GHz, Phys. Med. Biol. 50 (2005) 4711–4720.
[17] S. Keckeis, L. Wernecke, D.J. Salchow, N. Reichhart, O. Strauß, Activation of a Ca2+-dependent cation conductance with properties of TRPM2 by reactive oxygen species in lens epithelial cells, Exp. Eye Res. 161 (2017) 61–70.
[18] J.V. Greinera, T. Glonek, Hydrotropic function of ATP in the crystalline lens, Exp. Eye Res. 190 (2020) 107862–107867.
[19] E. Vaghefi, B.P. Pontre, M.D. Jacobs, P.J. Donaldson, Visualizing ocular lens fluid dynamics using MRI: manipulation of steady state water content and water fluxes, Am. J. Physiol. Regul. Integr. Comp. Physiol. 301 (2011) R335–R342.
[20] K.R. Heys, M.G. Friedrich, R.J.W. Truscott, Free and bound water in normal and cataractous human lenses, Invest. Ophthalmol. Vis. Sci. 49 (2008) 1991–1997.
[21] N. Pescosolido, A. Barbato, R. Giannotti, C. Komaiha, F. Lenarduzzi, Age-related changes in the kinetics of human lenses: prevention of the cataract, Int. J. Ophthalmol. 9 (2016) 1506–1517.
[22] E. Marzec, J. Olszewski, E. Grześkowiak, A. Kamińska, A. Bienert, K. Iwanik, Dielectric studies of the paracetamol-lenticular tissue interactions, Colloids Surf. B: Biointerfaces 84 (2011) 131–134.
[23] A. Abdel-Ghaffar, G.G. Elhossary, A.M. Mahmoud, A.H.M. Elshazly, O.A. Hassanin, A. Saleh, S.M. Mansour, F.G. Metwally, L.K. Hanafy, S.H. Karam, H. E. Amer, N.A. Samy, A.M. Ata, Potential prophylactic effect of chemical chaperones for alleviation of endoplasmic reticulum stress in experimental diabetic cataract, Bull. Natl. Res. Cent. 43 (2019) 71–86.
[24] R.H. Nagaraj, M. Linetsky, A.W. Stitt, The pathogenic role of Maillard reaction in the aging eye, Amino Acids 42 (2012) 1205–1220.
[25] D.K. Karumanchi, N. Karunaratne, L. Lurio, J.P. Dillon, E.R. Gaillard, Non–enzymatic glycation of α–crystallin as an in vitro model for aging, diabetes and degenerative diseases, Amino Acids 47 (2015) 2601–2608.
[26] M.K.N.S. Varsha, T. Raman, R. Manikandan, Inhibition of diabetic-cataract by vitamin K1 involves modulation of hyperglycemia-induced alterations to lens calcium homeostasis, Exp. Eye Res. 128 (2014) 73–82.
[27] J.C. Lim, R.D. Perwick, B. Li, P.J. Donaldson, Comparison of the expression and spatial localization of glucose transporters in the rat, bovine and human lens, Exp. Eye Res. 161 (2017) 193–204.
[28] E. Marzec, P. Sosnowski, J. Olszewski, H. Krauss, K. Bahloul, W. Samborski, A. Krawczyk-Wasielewska, Dielectric relaxation of normothermic and hypothermic rat corneas, Bioelectrochemistry 101 (2015) 132–137.
[29] B.A. Moffat, J.M. Pope, Anisotropic water transport in the human eye lens studied by diffusion tensor NMR micro-imaging, Exp. Eye Res. 74 (2002) 677–687.
[30] C.E. Jones, J.M. Pope, Measuring optical properties of an eye lens using magnetic resonance imaging, Magn. Reson. Imag. 22 (2004) 211–220.
[31] E. Vaghefi, B. Pontre, P.J. Donaldson, P.J. Hunter, M.D. Jacobs, Visualization of transverse diffusion paths across fiber cells of the ocular lens by small animal MRI, Physiol. Meas. 30 (2009) 1061–1073.
[32] P.J. Donaldson, A.C. Grey, B. Maceo Heilman, J.C. Lim, E. Vaghefi, The physiological optics of the lens, Prog. Retin. Eye Res. 56 (2017) e1–e24.
[33] K. Sasaki, I. Popov, Y. Feldman, Water in the hydrated protein powders: dynamic and structure, J. Chem. Phys. 150 (2019) 204504–204511.
[34] S.M. Lee, S.Y. Lin, C.L. Cheng, R.C. Liang, Possible changes in secondary structure and composition of human lens capsules in hereditary congenital cataract, Graefe's Arch. Clin. Exp. Ophthalmol. 234 (1996) 342–348.
[35] S. Mukhopadhyay, M. Kar, K.P. Das, Effect of methylglyoxal modification of human alpha-crystallin on the structure, stability and chaperone function, Protein J. 29 (2010) 551–556.
[36] R.H. Nagaraj, I.N. Shipanova, F.M. Faust, Protein cross-linking by the Maillard reaction. Isolation, characterization, and in vivo detection of a lysine-lysine cross-link derived from methylglyoxal, J. Biol. Chem. 271 (1996) 19338–19345.
[37] S. Swamy-Mruthinti, S.M. Shaw, H.R. Zhao, K. Green, E.C. Abraham, Evidence of a glycemic threshold for the development of cataracts in diabetic rats, Curr. Eye Res. 18 (1999) 423–429.
[38] E. Marzec, K. Wierzbicki, J. Olszewski, W. Samborski, E. Skorupska, K. Bahloul, A. Krzywicka, H. Krauss, Dielectric phenomena associated with the keratin-glucose interactions of nail plate, Colloids Surf. B: Biointerfaces 109 (2013) 143–146.
[39] A. Tarannum, J.R. Rao, N.N. Fathima, Stability of collagen in ionic liquids: ion specific Hofmeister series effect, Spectrochim. Acta A Mol. Biomol. Spectrosc. 212 (2019) 343–348.
[40] P.P. Fagerholm, B.T. Philipson, B. Lindstron, Normal human lens, the distribution of protein, Exp. Eye Res. 33 (1981) 615–620.
[41] C. Slingsby, G.J. Wistow, A.R. Clark, Evolution of crystallins for a role in the vertebrate eye lens, Protein Sci. 22 (2013) 367–380.
[42] I. Rodríguez-Arteche, S. Cerveny, Á. Alegría, J. Colmenero, Dielectric spectroscopy in the GHz region on fully hydrated zwitterionic amino acids, Phys. Chem. Chem. Phys. 14 (2012) 11352–11362.
[43] V. Raicu, Y. Feldman, Dielectric relaxation in biological systems, Physical principles, methods, and applications, Oxford University Press, 2015.
[44] J. Horwitz, Alpha-crystallin, Exp. Eye Res. 76 (2003) 145–153.